YIC GACM 2015
3rd ECCOMAS Young Investigators Conference
6th GACM Colloquium
July 20–23, 2015, Aachen, Germany

Heat transfer in binary gas-mixtures confined in a square cavity

Vinay Kumar Gupta [a,*], Manuel Torrilhon [a]

[a] Center for Computational Engineering Science,
Department of Mathematics, RWTH Aachen University,
Schinkelstr. 2, D-52062 Aachen, Germany

*gupta@mathcces.rwth-aachen.de

Abstract. *Heat transfer in rarefied binary gas-mixtures confined in a bottom-heated squared cavity is investigated through the Grad's moment equations for gaseous mixtures composed of Maxwell molecules. The numerical method based on finite differences is presented and the convergence of the numerical method is studied. Some preliminary results on heat transfer are presented.*

Keywords: Boltzmann equation, binary gas-mixtures, bottom-heated cavity, Grad's moment equations

1 INTRODUCTION

Miniaturization of micro-devices further and further has become a popular trend in recent times, and it necessitates good-understanding of heat transfer mechanism in these devices for designing, fabricating and optimizing their performances. In micro-devices, it is quite common to have a hot plate surrounded by several other cold plates maintained at ambient temperature, and to close and package this system in vacuum. Rarefied (or non-rarefied) gases are usually present in the package and the heat transfer takes place from hot to cold plates leading to many rarefaction phenomena [1–4]. The heat transfer in a (bottom-)heated square cavity is a classical problem in fluid mechanics and has been studied by a few authors in context of single gases [1–4] and references therein. Unfortunately, we have not found any work in the existing literature on the same problem in context of gaseous mixtures.

Owing to size of micro-devices, the macroscopic length scale is of the order of mean-free path, and therefore, the Knudsen number, Kn—defined as the ratio of mean-free-path to a macroscopic length scale pertaining to problem—for micro devices is not small. Typically, the Knudsen number encountered in micro-devices ranges from 0.01 to 1 [5] which is amalgam of the typical range of the so-called slip-flow regime ($0.001 \lesssim \mathrm{Kn} \lesssim 0.1$) and transition regime ($0.1 \lesssim \mathrm{Kn} \lesssim 10$) [6]. Usually, the conventional fluid dynamical equations—e.g., Euler or Navier–Stokes and Fourier (NSF) equations—break down in describing processes in these regimes. For describing processes in the slip-flow regime, the NSF equations equipped with appropriate velocity slip and temperature jump boundary conditions may still be acceptable [6, 7]; however, they are not adequate for flow descriptions in the transition regime [6]. Moreover, particle-based methods, such as direct simulation Monte-Carlo (DSMC) and discrete velocity methods, are forbiddingly expensive in the transition regime. The moment equations derived from the Boltzmann equation—which is capable of describing processes in any regime but is extremely difficult to solve analytically and is computationally very expensive to solve numerically if discretized directly—offer an attractive alternative for describing the processes in the transition regime with reasonable compromise between computational cost and numerical accuracy.

In this paper, we consider the problem of heat transfer in binary noble gas-mixtures confined in a square cavity whose bottom wall is heated while all other walls are at a constant colder temperature, and study it numerically through the Grad's 2×13-moment ($2\times$G13) equations for binary mixtures of monatomic-inert-ideal gases—interacting with Maxwell interaction potential (or made up of Maxwell molecules (MM)).

2 PROBLEM DESCRIPTION AND METHOD OF SOLUTION

2.1 Problem description

We consider a binary mixture of gases α and β in steady state confined in a square cavity of side length L. Let the temperature of the bottom of the cavity be $T_H = T_\circ + \varepsilon \tilde{T}_H$ while the temperatures of its all other sides be $T_C = T_\circ$, where ε is a small parameter used also in the linearization, see [8]. The temperature difference between the hot wall and any cold wall of the cavity $T_H - T_C = \varepsilon \tilde{T}_H$ is taken very small in comparison to $T_\circ$ so that the linearized equations and linearized boundary conditions are sufficient for the description of the process. The schematic of the problem is shown in Figure 1. The third dimension z of the cavity is assumed very long so that the heat transfer essentially takes place in two dimensions (x and y) and, thus, z-axis in Figure 1 is just for illustration purposes.

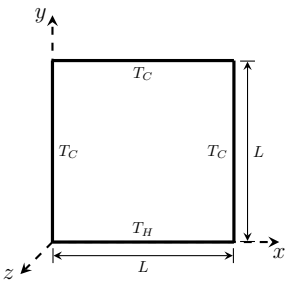

Figure 1: Schematic of a two-dimensional bottom heated square cavity; $T_H > T_C$.

2.2 Governing equations and boundary conditions

We shall study the problem via linear-dimensionless 2×G13 equations and associated boundary conditions derived from Maxwell accommodation model. The linear-dimensionless for 2×G13 equations follow from Equations (4.3)–(4.7) and (4.15) of [8], on considering them for both the constituent in the mixture and substituting $\hat{m}^{(\gamma)}_{ijk} = \hat{\Delta}_\gamma = 0$, $\hat{u}^{1(\gamma)}_{ij} = 7\hat{\sigma}^{(\gamma)}_{ij}$ for $\gamma \in \{\alpha, \beta\}$. For the sake of conciseness, we shall not present these equations here and the reader is referred to [8] for their detailed derivation, linearization, scaling and other notations, and to [9, 10] for understanding the computation of the production terms (right-hand sides) of these equations. Moreover, we shall also drop the hats over the dimensionless quantities for better readability and, therefore, in what follows, the quantities will understood dimensionless unless otherwise stated. The associated boundary conditions from the Maxwell accommodation model read ($\gamma \in \{\alpha, \beta\}$)

$$\left.\begin{aligned} u^{(\gamma)}_x(0,y) = u^{(\gamma)}_x(1,y) = u^{(\gamma)}_y(x,0) = u^{(\gamma)}_y(x,1) = 0, \\ \sigma^{(\gamma)}_{nt} = -\mathfrak{n}\frac{\chi_\gamma}{2-\chi_\gamma}\sqrt{\frac{2}{\pi}}\left[\frac{v_\circ}{\sqrt{\theta^\circ_\gamma}}\big(v_t - v_w\big) + \frac{1}{2}u^{(\gamma)}_t + \frac{1}{5}q^{(\gamma)}_t\right], \\ q^{(\gamma)}_n = -\mathfrak{n}\frac{\chi_\gamma}{2-\chi_\gamma}\sqrt{\frac{2}{\pi}}\left[2\big(T_\gamma - T_w\big) + \frac{1}{2}\sigma^{(\gamma)}_{nn}\right], \end{aligned}\right\} \tag{1}$$

where $\mathfrak{n} = 1$ for left and bottom walls while $\mathfrak{n} = -1$ for right and top walls; $n = x$ and $t = y$ for the left and right walls of the cavity whereas $n = y$ and $t = x$ for the bottom and top walls of the cavity; v_w, T_w denote the dimensionless perturbations in velocity and temperature, respectively, of a wall of the cavity from their respective dimensionless ground state values. For the present problem, $v_w = 0$ for all the walls, and $T_w = 0$ for the left, right and top walls while $T_w = T_H$ for the bottom wall where T_H is now scaled with $T_\circ$.

2.3 Numerical method

Owing to symmetry, we include the balance equations for both the diffusion velocities into the moment system (2×G13 equations and boundary conditions) while discard the total momentum balance equation. Furthermore, to get rid of the macroscopic velocity of the mixture (v_i), we replace the diffusion velocities of the constituents and the macroscopic velocity of the mixture in the moment system in terms of the individual macroscopic velocities $v^{(\alpha)}_i$ and $v^{(\beta)}_i$—by using the definitions of the diffusion velocities and macroscopic velocity of the mixture.

The linear-dimensionless 2×G13 equations can now be written as

$$P_1\,\partial_x \boldsymbol{U} + P_2\,\partial_y \boldsymbol{U} + R\,\boldsymbol{U} = \boldsymbol{0}, \tag{2}$$

where P_1, P_2 and R are constant matrices and $\boldsymbol{U}$ is the vector containing all the unknowns

$$\boldsymbol{U} = \left\{n_\alpha, v_x^{(\alpha)}, v_y^{(\alpha)}, T_\alpha, \sigma_{xx}^{(\alpha)}, \sigma_{xy}^{(\alpha)}, \sigma_{yy}^{(\alpha)}, q_x^{(\alpha)}, q_y^{(\alpha)}, n_\beta, v_x^{(\beta)}, v_y^{(\beta)}, T_\beta, \sigma_{xx}^{(\beta)}, \sigma_{xy}^{(\beta)}, \sigma_{yy}^{(\beta)}, q_x^{(\beta)}, q_y^{(\beta)}\right\}^\top.$$

We now discretize the dimensionless spatial domain of the cavity into $N_x \times N_y$ identical cells using the equispaced grid points $x_i = i\,\Delta x$ and $y_j = j\,\Delta y$ where $i = 0, 1, \ldots, N_x$ and $j = 0, 1, \ldots, N_y$; clearly, $x_0 = 0$, $x_{N_x} = 1$, $y_0 = 0$ and $y_{N_y} = 1$. With this discretization, (2) at each point (x_i, y_j) for $i = 0, 1, \ldots, N_x$ and $j = 0, 1, \ldots, N_y$ takes the form

$$P_1(\partial_x \boldsymbol{U})_{i,j} + P_2(\partial_y \boldsymbol{U})_{i,j} + R\,\boldsymbol{U}_{i,j} = \boldsymbol{0}, \tag{3}$$

where $\boldsymbol{U}_{i,j} = \boldsymbol{U}(x_i, y_j)$, and $(\partial_x \boldsymbol{U})_{i,j}$ and $(\partial_y \boldsymbol{U})_{i,j}$ are the numerical approximations for the derivatives in (2) at point (x_i, y_j). Both x and y derivatives in (2) are approximated with the central difference scheme at interior grid points while with forward/backward schemes at the boundaries as follows:

$$(\partial_x \boldsymbol{U})_{i,j} = \begin{cases} \frac{U_{i+1,j} - U_{i,j}}{\Delta x} & \text{for} \quad (i,j) \in \{0\} \times \{0, 1, \ldots, N_y\}, \\ \frac{U_{i+1,j} - U_{i-1,j}}{2\,\Delta x} & \text{for} \quad (i,j) \in \{1, 2, \ldots, N_x - 1\} \times \{0, 1, \ldots, N_y\}, \\ \frac{U_{i,j} - U_{i-1,j}}{\Delta x} & \text{for} \quad (i,j) \in \{N_x\} \times \{0, 1, \ldots, N_y\} \end{cases} \tag{4}$$

and

$$(\partial_y \boldsymbol{U})_{i,j} = \begin{cases} \frac{U_{i,j+1} - U_{i,j}}{\Delta y} & \text{for} \quad (i,j) \in \{0, 1, \ldots, N_x\} \times \{0\}, \\ \frac{U_{i,j+1} - U_{i,j-1}}{2\,\Delta y} & \text{for} \quad (i,j) \in \{0, 1, \ldots, N_x\} \times \{1, 2, \ldots, N_y - 1\}, \\ \frac{U_{i,j} - U_{i,j-1}}{\Delta y} & \text{for} \quad (i,j) \in \{0, 1, \ldots, N_x\} \times \{N_y\}. \end{cases} \tag{5}$$

The boundary conditions at each wall are applied by replacing the moment equation for a variable—for which one need to apply the boundary condition—with the corresponding boundary condition in discretized form. Combining all the discrete vectors $\boldsymbol{U}_{i,j}$'s into a vector $\boldsymbol{X} = \left\{\boldsymbol{U}_{i,j} | (i,j) \in \{0, 1, \ldots, N_x\} \times \{0, 1, \ldots, N_y\}\right\}^\top$, the full discretized moment system can again be written in form of $\mathcal{A}\boldsymbol{X} = \boldsymbol{b}$ where $\boldsymbol{b}$ is a constant vector and $\mathcal{A}$ is a constant matrix. The algebraic system, $\mathcal{A}\boldsymbol{X} = \boldsymbol{b}$, can then be solved for $\boldsymbol{X}$ using any standard iterative method, such as Gauss-Seidel method, for solving a linear system of equations.

3 RESULTS

In order to investigate the convergence of the numerical method, we choose the error in L^1-norm, defined as

$$\|\text{err}(\psi)\|_1 = \sum_{i=0}^{N_x} \sum_{j=0}^{N_y} \Delta x\,\Delta y\,\left|\psi^{(\text{ex})}(x_i, y_j) - \psi_{i,j}^{(\text{num})}\right|, \tag{6}$$

where ψ is any field variable and superscripts "(ex)" and "(num)" refer to exact and numerical solutions, respectively. We shall approximate the exact solution with a reference numerical solution obtained with 512×512 cells.

As an example, we consider neon–argon (Ne–Ar) mixture confined in the cavity. Let $T_H = 0.1$, $T_C = 0$, the mole fraction of Ne in the mixture be $\mathrm{x}_{\mathrm{Ne}}^{\circ} = 0.25$ and the accommodation coefficients be $\chi_\alpha = \chi_\beta = 1$. Figure 2 illustrates the errors in number densities of the constituents in L^1-norm on $\log_{10}$-$\log_{10}$ scale for different cell numbers $N_x \times N_y \in \{16 \times 16, 32 \times 32, 64 \times 64, 128 \times 128\}$ and for Knudsen numbers $\mathrm{Kn} = 0.01, 0.1$. It can be seen from Figure 2 that for very small Knudsen number (red lines) the method is second order convergent whereas for large Knudsen number (blue lines) the method is not second order convergent but is slightly more than first order convergent. This essentially happens due to the discretization at the walls which was first order accurate.

Figure 3 illustrates the velocity streamlines superposed over temperature contours on the left panel and heat flux lines plotted over the shear stress contours on the right panel, both for Ne gas in the mixture at $\mathrm{Kn} = 0.01$ with 100×100 cells. The values of other parameters are same as those for Figure 2. The left sub-figure of Figure 3 shows four (two primary and two secondary) antipodal-rotating vortices, symmetrical about yz-plane passing through the center of the cavity. The primary vortices are induced due to acute temperature differences at the lower corners of the cavity leading to thermal transpiration. The right sub-figure of Figure 3 depicts that the shear stress is almost zero in the whole cavity except at the lower corners where the acute temperature differences are present.

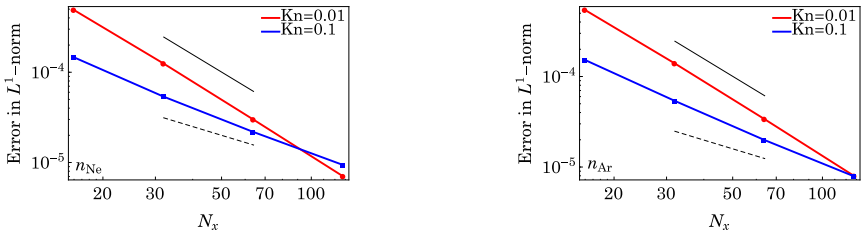

Figure 2: Empirical error in number densities of (left) Ne and (right) Ar in Ne–Ar mixture for different Knudsen numbers. The continuous and dashed black lines have the slopes of -2 and -1, respectively.

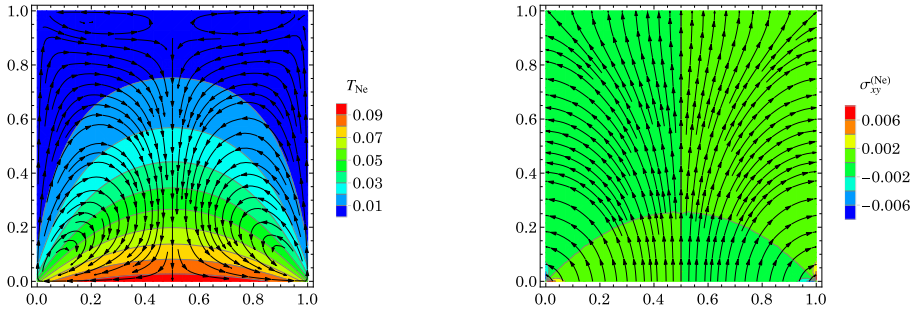

Figure 3: (Left) Velocity streamlines and temperature contours (right) heat flux lines and shear stress contours for Ne at $\mathrm{Kn} = 0.01$.

4 CONCLUSIONS

The numerical method for solving a two-dimensional problem of bottom heated cavity through $2\times$G13 equations is described and some preliminary results have been presented. Apparently, the Grad's moment equations for mixtures are a promising alternative to the computationally expensive methods, especially in the transition regime, for exploring different problems—at least qualitatively.

REFERENCES

[1] Y. Sone. Flows induced by temperature fields in a rarefied gas and their ghost effect on the behavior of a gas in the continuum limit. *Annu. Rev. Fluid Mech.*, **32**:779–811, 2000.

[2] Y. Sone. *Kinetic Theory and Fluid Dynamics*. Birkhäuser, Boston, 2002.

[3] C. Cai. Heat transfer in vacuum packaged microelectromechanical system devices. *Phys. Fluids*, **20**:017103, 2008.

[4] A. S. Rana, A. Mohammadzadeh, and H. Struchtrup. A numerical study of the heat transfer through a rarefied gas confined in a microcavity. *Continuum Mech. Thermodyn.*, **27**:433–446, 2015.

[5] W.-M. Zhang, G. Meng, and X. Wei. A review on slip models for gas microflows. *Microfluid. Nanofluid.*, **13**:845–882, 2012.

[6] H. Struchtrup. *Macroscopic Transport Equations for Rarefied Gas Flows*. Springer, Berlin, 2005.

[7] S. Colin. Gas microflows in the slip flow regime: A critical review on convective heat transfer. *J. Heat Transfer*, **134**:020908, 2012.

[8] V. K. Gupta and M. Torrilhon. Higher order moment equations for rarefied gas mixtures. *Proc. Roy. Soc. A*, **471**:20140754, 2015.

[9] V. K. Gupta and M. Torrilhon. Comparison of relaxation phenomena in binary gas-mixtures of Maxwell molecules and hard spheres. *Comput. Math. Appl.*, **70**:73–88, 2015.

[10] V. K. Gupta and M. Torrilhon. Automated Boltzmann collision integrals for moment equations. volume 1501 of *AIP Conference Proceedings*, pages 67–74, 2012.